

# Assignment in The Finite Element Method, FHLF01

Lukas Gardberg

May 2020

## 1 Introduction

This project consists of modelling an integrated circuit by creating a finite element program in MATLAB and solving three different types of boundary value problems. The subproblems are as follows:

1. Find the stationary temperature when the circuit is in an environment with temperature  $T_\infty = 18^\circ\text{C}$  and the heat generated in the die being  $Q = 5 \cdot 10^7 \text{ W/m}^3$ . Additionally, find the heat distribution with a 25% reduction in data consumption, and present the maximum temperature before and after.
2. Determine how the temperature distribution changes with respect to time during the first 20 minutes, and then find the stationary temperature distribution. What is the peak temperature for full and reduced data consumption?
3. Determine the effective von Mises stress field and the corresponding displacement field due to thermal expansion from the stationary temperature distribution. Investigate the effect of reduced data consumption. Present the stress distributions and displacement fields. What are the peak stresses and where are they found?

The heat in the die of the circuit is assumed to be proportional to the data, i.e.  $Q \propto \text{data}$ . It is assumed that the heat generation takes place inside the die in the middle of the integrated circuit. The simplified model of the integrated circuit consists of three different components made from different materials. The package is made from silver (Ag) filled epoxy, the die is made from silicon (Si) and the conducting frame is made from copper (Cu) (see figure 1).

### 1.1 Geometry and boundary conditions

Figure 1 represents the geometry of a cross section of the circuit as well as its boundary conditions. It has a thickness of  $t = 0.01 \text{ m}$ , and is mounted on a board, which results in  $u_x = 0, u_y = 0$  at the bottom of the copper section (see figure). Here  $u$  is the displacement. Because the problem is symmetric one can consider only the right part of the geometry, and therefore the boundary condition  $u_x = 0$  along the symmetry line has to be adopted. Additionally, a fan cools the circuit from above resulting in Newton convection along the top boundary. The rest of the boundaries are thermally insulated, and the circuit has an initial temperature of  $T_0 = 30^\circ\text{C}$ .

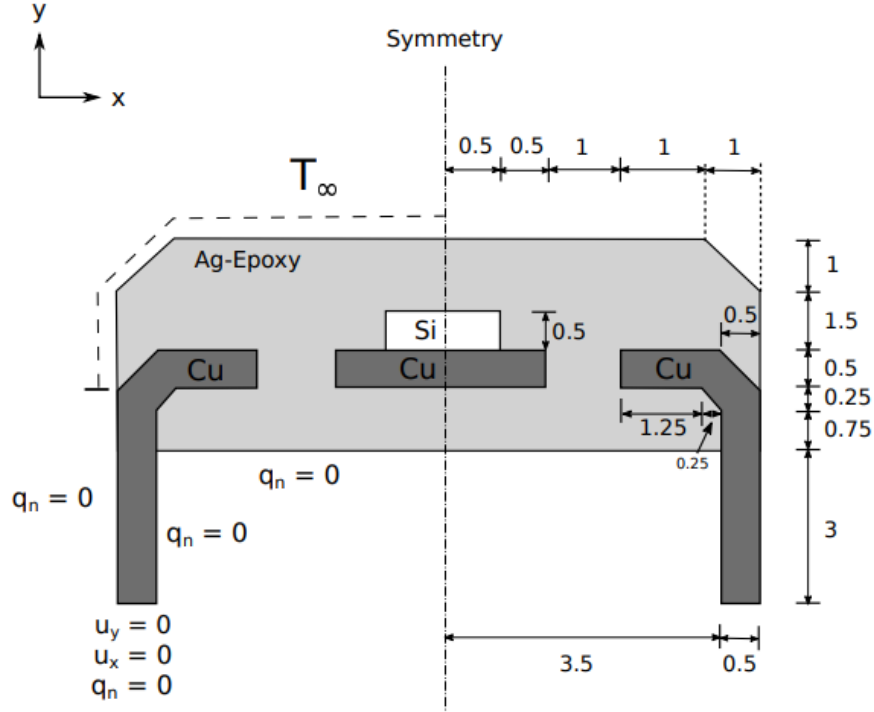


Figure 1: Sketch of a cross section of the integrated circuit. The boundary conditions and dimensions are symmetric around the symmetry line. All dimensions are in mm.

Below is a table of the material data relevant to the three sub problems.

	Ag-epoxy	Silicon	Copper
Young's modulus, $E$ [GPa]	7	165	128
Poisson's ratio, $\nu$ [-]	0.3	0.22	0.36
Expansion coefficient, $\alpha$ [1/K]	$4 \cdot 10^{-5}$	$2.6 \cdot 10^{-6}$	$17.6 \cdot 10^{-6}$
Density, $\rho$ [kg/m <sup>3</sup> ]	2500	2530	8930
Specific heat, $c_p$ [J/(kg K)]	1000	703	386
Thermal conductivity, $k$ [W/(m K)]	5	149	385

Table 1: Material data

## 2 Procedure

### 2.1 Heat Flow

For our considered body  $A$  it is apparent that the heat that is transferred into the body is equal to the heat that is transferred out of it (the conservation principle) [1]. This means that

$$\int_A Q t \, dA = \oint_{\mathcal{L}} q_n t \, d\mathcal{L}. \quad (1)$$

Here  $Q$  is the internal heat supply,  $t$  the thickness of the body,  $q_n$  the heat flux perpendicular to the boundary, and  $\mathcal{L}$  the boundary of  $A$ . Using **Gauss' divergence theorem**, which states that

$$\int_A \operatorname{div} \mathbf{q} \, dA = \oint_{\mathcal{L}} \mathbf{q}^T \mathbf{n} \, d\mathcal{L}, \quad (2)$$

together with (1) results in

$$\operatorname{div}(t\mathbf{q}) = tQ. \quad (3)$$

Using this constitutive relation we can write the flow vector as

$$\mathbf{q} = -\mathbf{D}\nabla T \quad (4)$$

where  $\mathbf{D}$  is the *constitutive matrix*, containing information of how easily heat flows in different directions. For two dimensional heat flow in one of our materials  $i$  we have that

$$\mathbf{D} = \begin{bmatrix} k_i & 0 \\ 0 & k_i \end{bmatrix}$$

where  $k_i$  is the corresponding thermal conductivity constant. Inserting (4) into (3) we get

$$\operatorname{div}(t\mathbf{D}\nabla T) + tQ = 0 \quad (5)$$

which is the first part of the strong form of two dimensional heat flow. What remains are the boundary conditions. These are formulated as

$$q_n = \mathbf{q}^T \mathbf{n} = h \quad \text{on } \mathcal{L}_h, \quad T = g \quad \text{on } \mathcal{L}_g. \quad (6)$$

The boundary on which the flux is known is denoted by  $\mathcal{L}_h$ , and the part on which the temperature is known is denoted by  $\mathcal{L}_g$ . The flux parallel to the normal of the boundary  $\mathcal{L}_g$  is denoted by  $q_n$ , and lastly  $g$  the temperature on the boundary  $\mathcal{L}_h$ . In the case when convection exists, we have that the flux is proportional to the difference of the temperature on the boundary, i.e

$$q_n = \alpha_c(T - T_\infty) \quad (7)$$

where  $\alpha_c = 40 \text{ W}/(\text{m}^2 \text{ K})$  is a proportionality constant,  $T$  the temperature on the boundary and  $T_\infty$  the surrounding temperature (assumed constant).

In order to obtain the FE-formulation for our problem, we first need to obtain the weak form. By multiplying (3) with an arbitrary *weight function*  $v(x, y)$  and integrating over our body  $A$  we obtain

$$\int_A v \operatorname{div}(t\mathbf{q}) \, dA - \int_A vQt \, dA = 0. \quad (8)$$

Using the **Green-Gauss theorem**, which states that

$$\int_A \phi \operatorname{div} \mathbf{q} \, dA = \oint_{\mathcal{L}} \phi \mathbf{q}^T \mathbf{n} \, d\mathcal{L} - \int_A (\nabla \phi)^T \mathbf{q} \, dA, \quad (9)$$

the first integral in (8) becomes

$$\int_A v \operatorname{div}(\mathbf{q}t) \, dA = \oint_{\mathcal{L}} vt \mathbf{q}^T \mathbf{n} \, d\mathcal{L} - \int_A (\nabla v)^T \mathbf{q}t \, dA$$

which we insert into (8) and get

$$\int_A (\nabla v)^T \mathbf{q}t \, dA = \oint_{\mathcal{L}} v \mathbf{q}^T \mathbf{n}t \, d\mathcal{L} - \int_A vQt \, dA.$$

Using the boundary conditions specified in (6) as well as the constitutive relation (4) the weak formulation is obtained as

$$\begin{aligned} \int_A (\nabla v)^T t \mathbf{D} \nabla T \, dA &= - \int_{\mathcal{L}_h} vht \, d\mathcal{L} - \int_{\mathcal{L}_g} vq_n t \, d\mathcal{L} + \int_A vQt \, dA \\ T &= g \quad \text{on } \mathcal{L}_g \end{aligned} \quad (10)$$

(s. 85) In our application all boundaries are thermally insulated except for the top part, which is subject to convection. This means that  $q_n = 0$  on the insulated boundaries, which, together with (7), results in the weak form

$$\int_A (\nabla v)^T t \mathbf{D} \nabla T \, dA = - \int_{\mathcal{L}_h} v\alpha_c(T - T_\infty)t \, d\mathcal{L} + \int_A vQt \, dA \quad (11)$$

as we have no part of the boundary where the flux is unknown.

From this the finite element formulation can be derived. The temperature of the entire region is approximated as  $T(x, y) = \mathbf{N}\mathbf{a}$  where  $\mathbf{N}$  contains the global shape functions. Each function in  $\mathbf{N}$  is defined by

$$N_i(x, y) = \begin{cases} N_i^\alpha(x, y) & \text{if element } \alpha \text{ contains global nodal point } i \\ 0 & \text{otherwise} \end{cases}$$

where the element shape function  $N_i^e$  for an element  $e$  is defined by

$$N_i^e = \begin{cases} 1 & \text{at nodal point } i \\ 0 & \text{at all other nodal points} \end{cases}$$

Further,  $\mathbf{a}$  denotes the temperatures in the nodes, where both  $\mathbf{a}$  and  $\mathbf{N}$  have a length equal to the chosen number of nodes  $n_{nodes}$ . The matrix  $\mathbf{B} = \nabla \mathbf{N}$  is defined as well as  $\nabla T = \mathbf{B}\mathbf{a}$ . The choice of weight function is done using the Galerkin method with  $v = \mathbf{N}\mathbf{c}$ , where  $\mathbf{c}$  is arbitrary as  $v$  also is. We have that  $\nabla v = \mathbf{B}\mathbf{c}$  and as  $v$  is a scalar function  $v = \mathbf{c}^T \mathbf{N}^T$  (s.208). Inserting this into (11) results in

$$\mathbf{c}^T \left[ \left( \int_A \mathbf{B}^T \mathbf{D} \mathbf{B} t \, dA \right) \mathbf{a} + \int_{\mathcal{L}_h} \mathbf{N}^T \alpha_c (\mathbf{N}\mathbf{a} - T_\infty) t \, d\mathcal{L} - \int_A \mathbf{N}^T Q t \, dA \right] = 0.$$

Because this holds for arbitrary  $\mathbf{c}$ , the inner expression is equal to zero. Using this and splitting the integral over the boundary  $\mathcal{L}_h$  in two, with  $\mathcal{L}_c$  as our convective boundary, gives

$$\left( \int_A \mathbf{B}^T \mathbf{D} \mathbf{B} t dA + \int_{\mathcal{L}_c} \mathbf{N}^T \alpha_c \mathbf{N} t d\mathcal{L} \right) \mathbf{a} + \int_{\mathcal{L}_h} \mathbf{N}^T \alpha_c T_\infty t d\mathcal{L} - \int_A \mathbf{N}^T Q t dA = 0$$

which is the FE formulation for our problem. This can be written compactly as

$$(\mathbf{K} + \mathbf{K}_c) \mathbf{a} = \mathbf{f}_b + \mathbf{f}_l \quad (12)$$

with

$$\begin{aligned} \mathbf{K} + \mathbf{K}_c &= \int_A \mathbf{B}^T \mathbf{D} \mathbf{B} t dA + \int_{\mathcal{L}_h} \mathbf{N}^T \alpha_c \mathbf{N} t d\mathcal{L} \\ \mathbf{f}_b &= - \int_{\mathcal{L}_h} \mathbf{N}^T \alpha_c T_\infty t d\mathcal{L} \\ \mathbf{f}_l &= \int_A \mathbf{N}^T Q t dA \end{aligned} \quad (13)$$

where  $\mathbf{K}_c$  represents the convective part of the stiffness matrix. It is possible to calculate the stiffness matrix and the force vector element-wise, which is useful during the computer implementation. We then only consider the approximation  $T = \mathbf{N}^e \mathbf{a}^e$  where  $\mathbf{N}^e$  is the element shape function matrix for the specified element and  $\mathbf{a}^e$  the temperatures at the element nodes. From this we can obtain the FE formulation for one element as

$$\mathbf{K}^e \mathbf{a}^e = \mathbf{f}_b^e + \mathbf{f}_l^e$$

which for an element  $\alpha$  is defined by

$$\begin{aligned} \mathbf{K}^e &= \int_{A_\alpha} \mathbf{B}^{eT} \mathbf{D} \mathbf{B}^e t dA + \int_{\mathcal{L}_{h\alpha}} \mathbf{N}^{eT} \alpha_c \mathbf{N}^e t d\mathcal{L} \\ \mathbf{f}_b^e &= - \int_{\mathcal{L}_h} \mathbf{N}^{eT} \alpha_c T_\infty t d\mathcal{L} \\ \mathbf{f}_l^e &= \int_{A_\alpha} \mathbf{N}^{eT} Q t dA. \end{aligned} \quad (14)$$

These can then be assembled according to the structure of the chosen mesh in order to obtain the global stiffness matrix. [1]

For our element boundary force vector  $\mathbf{f}_b^e$  only two of the three element nodes, the ones on the boundary, are to be integrated over. If we wish to integrate from a node at  $x_1$  to  $x_2$  the element shape functions are

$$\mathbf{N}^e = [N_1^e \quad N_2^e] = \left[ -\frac{1}{L}(x - x_2) \quad \frac{1}{L}(x - x_1) \right]$$

where  $L = x_2 - x_1$  is the length of the interval. This implies that

$$\mathbf{f}_b^e = \alpha_c T_\infty t \int_{x_1}^{x_2} \mathbf{N}^{eT} dx = \alpha_c T_\infty t \begin{bmatrix} L/2 \\ L/2 \end{bmatrix}.$$

Similarly for the element stiffness matrix corresponding to convection we have that

$$\alpha_c T_\infty t \int_{\mathcal{L}_{h\alpha}} \mathbf{N}^e \mathbf{T} \mathbf{N}^e d\mathcal{L} = \alpha_c T_\infty t \int_{x_1}^{x_2} \begin{bmatrix} (N_1^\alpha)^2 & N_1^\alpha N_2^\alpha & 0 \\ N_2^\alpha N_1^\alpha & (N_2^\alpha)^2 & 0 \\ 0 & 0 & 0 \end{bmatrix} dx$$

which evaluates into

$$\frac{L}{6} \alpha_c T_\infty t \begin{bmatrix} 2 & 1 & 0 \\ 1 & 2 & 0 \\ 0 & 0 & 0 \end{bmatrix}.$$

This gives us the necessary means to solve (12).

## 2.2 Transient Heat Flow

In this section we consider a non-stationary heat distribution which evolves over time. An initial temperature of  $T_0 = 30^\circ\text{C}$  is assumed. The strong formulation of the problem is similar to (5) but with an additional time derivative term added, which results in

$$c_p \rho \dot{T} + \text{div}(\mathbf{D} \nabla T) + Q = 0$$

where  $c_p$  and  $\rho$  are the specific heat and the density of the material (see table 1). In the same way the weak form of the stationary heat flow problem was derived we multiply by an arbitrary weight function, integrate over our body, and make use of the Green-Gauss theorem which results in

$$\int_A (\nabla v)^T \mathbf{D} \nabla T dA = - \int_{\mathcal{L}_h} v \alpha_c (T - T_\infty) d\mathcal{L} + \int_A v Q dA + \int_A v c_p \rho \dot{T} dA$$

which is the weak form for the problem. Assigning  $v = \mathbf{N} \mathbf{c}$  and noting that  $\mathbf{c}$  can be chosen arbitrarily after insertion, analogously to deriving the FE formulation for the stationary problem, we obtain

$$\left( \int_A \mathbf{B}^T \mathbf{D} \mathbf{B} dA + \int_{\mathcal{L}_c} \mathbf{N}^T \alpha_c \mathbf{N} d\mathcal{L} \right) \mathbf{a} + \int_{\mathcal{L}_h} \mathbf{N}^T \alpha_c T_\infty d\mathcal{L} - \int_A \mathbf{N}^T Q dA + \int_A \mathbf{N}^T c_p \rho \mathbf{N} dA \dot{\mathbf{a}} = 0$$

with  $T = \mathbf{N} \mathbf{a}$ . Collecting the last integral in

$$\mathbf{C} = \int_A \mathbf{N}^T c_p \rho \mathbf{N} dA$$

results in the FE formulation

$$\mathbf{C} \dot{\mathbf{a}} + (\mathbf{K} + \mathbf{K}_c) \mathbf{a} = \mathbf{f}_b + \mathbf{f}_l. \quad (15)$$

Note that the time dependence is separated from the space dependence in the equation, as  $\mathbf{a} = \mathbf{a}(t)$ .

To obtain a solution for this problem, we have to solve it iteratively over time. For this a time-stepping scheme is needed. We use the simple approximation

$$\dot{\mathbf{a}} = \frac{\mathbf{a}(t_{n+1}) - \mathbf{a}(t_n)}{t_{n+1} - t_n}$$

We use the following approximations for the temperatures and the boundary forces

$$\begin{aligned}\mathbf{a} &= \theta \mathbf{a}_{n+1} + (1 - \theta) \mathbf{a}_n \\ \mathbf{f} &= \theta \mathbf{f}_{n+1} + (1 - \theta) \mathbf{f}_n\end{aligned}\tag{16}$$

Because  $\mathbf{f}$  does not depend on time  $\mathbf{f}_n = \mathbf{f}$  for all time steps  $n$ . Inserting these into (15) with  $\theta = 1$  (implicit time stepping) results in

$$(\mathbf{C} + \Delta t(\mathbf{K} + \mathbf{K}_c))\mathbf{a}_{n+1} = \mathbf{C}\mathbf{a}_n + \Delta t \mathbf{f}\tag{17}$$

which is our chosen time stepping method with  $\mathbf{a}_0$  having the value  $T_0$  in every node [2].

### 2.3 Stresses and strains

In order to obtain the strong form for two dimensional elasticity we first need to make a few definitions. The *traction vector*

$$\mathbf{t} = \begin{bmatrix} t_x \\ t_y \\ t_z \end{bmatrix}\tag{18}$$

represents an incremental force per unit area on the surface of the body, having the directional components  $t_x, t_y, t_z$  and the unit N/m<sup>2</sup>. Considering such a traction vector for each normal vector parallel to one of the axis x, y, and z, for example

$$\mathbf{s}_x = \begin{bmatrix} \sigma_{xx} \\ \sigma_{xy} \\ \sigma_{xz} \end{bmatrix}\tag{19}$$

which corresponds to the normal vector in the x-direction, we can collect these in a stress tensor

$$\mathbf{S} = \begin{bmatrix} \mathbf{s}_x^T \\ \mathbf{s}_y^T \\ \mathbf{s}_z^T \end{bmatrix} = \begin{bmatrix} \sigma_{xx} & \sigma_{xy} & \sigma_{xz} \\ \sigma_{yx} & \sigma_{yy} & \sigma_{yz} \\ \sigma_{zx} & \sigma_{zy} & \sigma_{zz} \end{bmatrix}\tag{20}$$

which contains all of our stress components. One important property of this matrix is that

$$\mathbf{S} = \mathbf{S}^T$$

which lowers the number of potentially unknown stresses from 9 to 6. Additionally to this we have a body force vector  $\mathbf{b}^T = [b_x \ b_y \ b_z]$  which in our case is equal to the zero vector since no outer forces are acting on our body.

The usefulness of the stress tensor becomes apparent when we note that the traction vector in any direction  $\mathbf{n}^T = [n_x \ n_y \ n_z]$  can be expressed as

$$\mathbf{t} = \mathbf{S}\mathbf{n}.$$

Now considering equilibrium for an arbitrary part of our body  $A$  yields

$$\int_{\mathcal{L}} \mathbf{t} \, d\mathcal{L} = \mathbf{0}$$

which, if we split into its directional components and use Gauss' divergence theorem results in

$$\begin{aligned}\frac{\partial \sigma_{xx}}{\partial x} + \frac{\partial \sigma_{xy}}{\partial y} + \frac{\partial \sigma_{xz}}{\partial z} &= 0 \\ \frac{\partial \sigma_{yx}}{\partial x} + \frac{\partial \sigma_{yy}}{\partial y} + \frac{\partial \sigma_{yz}}{\partial z} &= 0 \\ \frac{\partial \sigma_{zx}}{\partial x} + \frac{\partial \sigma_{zy}}{\partial y} + \frac{\partial \sigma_{zz}}{\partial z} &= 0\end{aligned}\tag{21}$$

which can be compactly written as

$$\tilde{\nabla}^T \boldsymbol{\sigma} = \mathbf{0}\tag{22}$$

with the definitions

$$\tilde{\nabla}^T = \begin{bmatrix} \frac{\partial}{\partial x} & 0 & 0 & \frac{\partial}{\partial y} & \frac{\partial}{\partial z} & 0 \\ 0 & \frac{\partial}{\partial y} & 0 & \frac{\partial}{\partial x} & 0 & \frac{\partial}{\partial z} \\ 0 & 0 & \frac{\partial}{\partial z} & 0 & \frac{\partial}{\partial x} & \frac{\partial}{\partial y} \end{bmatrix}; \quad \boldsymbol{\sigma} = \begin{bmatrix} \sigma_{xx} \\ \sigma_{yy} \\ \sigma_{zz} \\ \sigma_{xy} \\ \sigma_{xz} \\ \sigma_{yz} \end{bmatrix}\tag{23}$$

which represents the balance principle for our body, where  $\boldsymbol{\sigma}$  are the sought after stresses for each element. Because plain strain conditions hold, we have that  $\sigma_{xz} = \sigma_{yz} = 0$ , leaving the only stress involving  $z$  to be  $\sigma_{zz}$  which can be calculated as

$$\sigma_{zz} = \nu(\sigma_{xx} + \sigma_{yy}) - \alpha E \Delta T$$

where the constants are defined in Table 1 and  $\Delta T$  is the mean calculated temperature over the element. [1] (p. 256) Because of this we can reduce the definition of the stress tensor and the ones in (23) to

$$\tilde{\nabla}^T = \begin{bmatrix} \frac{\partial}{\partial x} & 0 & \frac{\partial}{\partial y} \\ 0 & \frac{\partial}{\partial y} & \frac{\partial}{\partial x} \end{bmatrix}; \quad \boldsymbol{\sigma} = \begin{bmatrix} \sigma_{xx} \\ \sigma_{yy} \\ \sigma_{xy} \end{bmatrix}; \quad \mathbf{S} = \begin{bmatrix} \sigma_{xx} & \sigma_{xy} \\ \sigma_{yx} & \sigma_{yy} \end{bmatrix}.\tag{24}$$

Now let's consider the resulting deformation of the body, i.e. the strain. The displacement vector

$$\mathbf{u} = \begin{bmatrix} u_x \\ u_y \end{bmatrix}\tag{25}$$

represents the displacement for a certain point on the body caused by the deformation relative to the original position, where the  $z$  component is zero in the plane strain case. From this we can define the *normal strain* as

$$\varepsilon_{xx} = \frac{\partial u_x}{\partial x}; \quad \varepsilon_{yy} = \frac{\partial u_y}{\partial y}\tag{26}$$

which represents the relative elongation. Here we have assumed that the displacement gradients are small. We can also define the *shear strain* as

$$\gamma_{xy} = \frac{\partial u_x}{\partial y} + \frac{\partial u_y}{\partial x}$$

which represents a change in angle between coordinate directions  $x$  and  $y$ . Collecting these strains in a vector

$$\boldsymbol{\epsilon} = \begin{bmatrix} \epsilon_{xx} \\ \epsilon_{yy} \\ \gamma_{xy} \end{bmatrix}$$



we can express it as

$$\boldsymbol{\epsilon} = \tilde{\nabla} \mathbf{u}$$

where

$$\tilde{\nabla} = \begin{bmatrix} \frac{\partial}{\partial x} & 0 \\ 0 & \frac{\partial}{\partial y} \\ \frac{\partial}{\partial y} & \frac{\partial}{\partial x} \end{bmatrix}.$$

The relation between stresses and strains is called a constitutive relation. Such a linear elastic relation

$$\boldsymbol{\sigma} = E \boldsymbol{\epsilon}$$

is called *Hooke's law* (boken s. 248) where  $E$  is Young's modulus defined in table 1. If we assume linear elasticity we can express the relation for all stresses and strains as

$$\boldsymbol{\sigma} = \mathbf{D} \boldsymbol{\epsilon}$$

where  $\mathbf{D}$  contains the linear elastic relations for each element related to the material. An important note is that if we have *thermal strains* zero stresses does not imply zero strains. These strains are caused by the thermal expansion of the material, resulting in

$$\boldsymbol{\sigma} = \mathbf{D} \boldsymbol{\epsilon} - \mathbf{D} \boldsymbol{\epsilon}_0 \quad (27)$$

where  $\boldsymbol{\epsilon}_0$  represents the thermal strains in the planar case as

$$\boldsymbol{\epsilon}_0 = (1 + \nu) \alpha \Delta T \begin{bmatrix} 1 \\ 1 \\ 0 \end{bmatrix} \quad (28)$$

and the constitutive matrix [1] (p. 235 - 256)

$$\mathbf{D} = \frac{E}{(1 + \nu)(1 - 2\nu)} \begin{bmatrix} 1 - \nu & \nu & 0 \\ \nu & 1 - \nu & 0 \\ 0 & 0 & \frac{1}{2}(1 - 2\nu) \end{bmatrix}. \quad (29)$$

## 2.4 Weak form & FE formulation

To obtain the weak form of our problem we first consider (21) and multiply by a vector of weight functions

$$\mathbf{v} = \begin{bmatrix} v_x \\ v_y \end{bmatrix}$$

The next step is to integrate over our body, and transfer over the  $\tilde{\nabla}$  operator to the weight vector via partial integration. Leaving out some detail, we finally use the Green-Gauss theorem, analogously to earlier weak formulations, to obtain

$$\int_A (\tilde{\nabla} \mathbf{v})^T \boldsymbol{\sigma} t \, dA = \oint_{\mathcal{L}} \mathbf{v}^T \mathbf{t} t \, d\mathcal{L} \quad (30)$$

where  $t$  is the thickness of the body, and  $\mathbf{t}$  the earlier defined traction vector in two dimensions. Adopting the approximations

$$\mathbf{u} = \mathbf{N} \mathbf{a}, \quad \mathbf{v} = \mathbf{N} \mathbf{c},$$

similarly to the FE formulation for heat flow in section 2.1 but now with a different form for  $\mathbf{c}$  as  $\mathbf{v}$  is a vector. This gives  $\tilde{\mathbf{V}}\mathbf{v} = \mathbf{B}\mathbf{c}$  with  $\mathbf{B} = \tilde{\mathbf{V}}\mathbf{N}$ . Inserted into (30) we obtain the weak form as

$$\int_A \mathbf{B}^T \boldsymbol{\sigma} t \, dA = \oint_{\mathcal{L}} \mathbf{N}^T \mathbf{t} t \, d\mathcal{L} \quad (31)$$

since the equation must hold for arbitrary  $\mathbf{c}$  (just like earlier). Now we introduce the effects of the material. We insert (27) into (31) and use that  $\boldsymbol{\epsilon} = \mathbf{B}\mathbf{a}$  which gives

$$\left( \int_A \mathbf{B}^T \mathbf{D} \mathbf{B} t \, dA \right) \mathbf{a} = \oint_{\mathcal{L}} \mathbf{N}^T \mathbf{t} t \, d\mathcal{L} + \int_A \mathbf{B}^T \mathbf{D} \boldsymbol{\epsilon}_0 t \, dA \quad (32)$$

The boundary conditions for the problem can be stated as

$$\mathbf{t} = \mathbf{S}\mathbf{n} = \mathbf{h} \quad \text{on } \mathcal{L}_h, \quad \mathbf{u} = \mathbf{g} \quad \text{on } \mathcal{L}_g,$$

where  $\mathcal{L}_h$  is where the traction is known,  $\mathcal{L}_g$  is where the displacement is known, and  $\mathcal{L}_h + \mathcal{L}_g = \mathcal{L}$ . However, there are no loads ( $\mathbf{t} = \mathbf{0}$ ) on all parts of the boundary where the chip is not mounted and the displacement is zero. This makes our boundary load vector zero, thus resulting in the formulation  $\mathbf{K}\mathbf{a} = \mathbf{f}_0$  with

$$\begin{aligned} \mathbf{K} &= \int_A \mathbf{B}^T \mathbf{D} \mathbf{B} t \, dA \\ \mathbf{f}_0 &= \int_A \mathbf{B}^T \mathbf{D} \boldsymbol{\epsilon}_0 t \, dA \end{aligned} \quad (33)$$

Similarly to the section prior an FE formulation for a single element is also sought after, which takes the form

$$\begin{aligned} \mathbf{K}^e &= \int_A \mathbf{B}^{eT} \mathbf{D} \mathbf{B}^e t \, dA \\ \mathbf{f}_0^e &= \int_A \mathbf{B}^{eT} \mathbf{D} \boldsymbol{\epsilon}_0 t \, dA \end{aligned} \quad (34)$$

This formulation can then be used element-wise to obtain the global formulation by assembling the element matrices according to the structure of the mesh. [1] (p. 299 - 306)

When obtaining the stresses and the strains by solving our finite element equation it can be of value to assert if a permanent deformation has occurred (yield stress) or if the material has fractured. This is done by evaluating when a function  $F(\boldsymbol{\sigma}; \sigma_s) = 0$ , where  $\boldsymbol{\sigma}$  is our stresses defined in (24) and  $\sigma_s$  our yield stress, which is a critical point of when deformation occurs. The functions  $F$  varies, but it's purpose is to give a measure of the total stress which an element is subject to. Specifically we consider the Von Mises stress field

$$\sigma_{eff} = \sqrt{\sigma_{xx}^2 + \sigma_{yy}^2 + \sigma_{zz}^2 - \sigma_{xx}\sigma_{yy} - \sigma_{xx}\sigma_{zz} - \sigma_{yy}\sigma_{zz} + 3\sigma_{xy}^2}. \quad (35)$$

which is evaluated for each element. [3]. We have that  $\sigma_{xz} = \sigma_{yz} = 0$  because of plain strain conditions [1] (p. 256). With the application of Von Mises stress field our function  $F$  becomes

$$F(\boldsymbol{\sigma}; \sigma_s) = \sigma_{eff} - \sigma_s$$

where  $\sigma_s$  can be looked up for the specific material.

### 3 Results

To start a rough mesh was made using 'pdetool' in MATLAB, which later was refined. The refined mesh can be seen in figure (2). This mesh was then used in solving the respective problems.

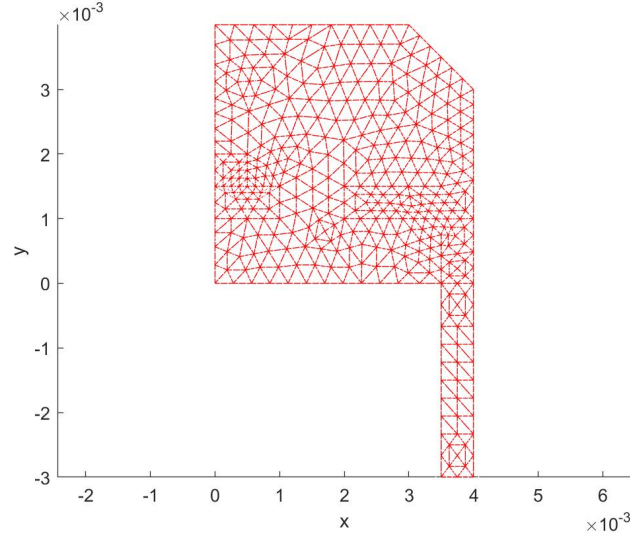
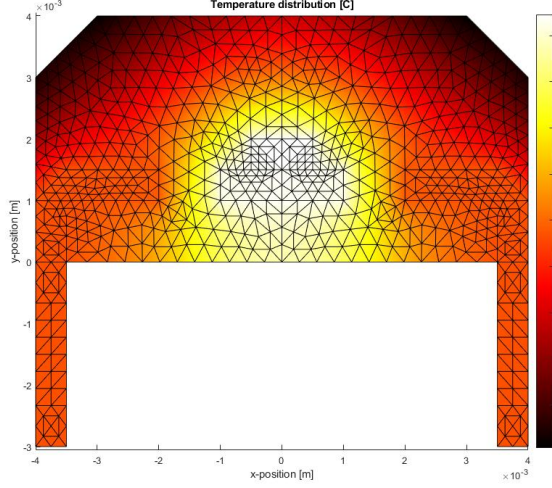


Figure 2: Mesh of modelled circuit

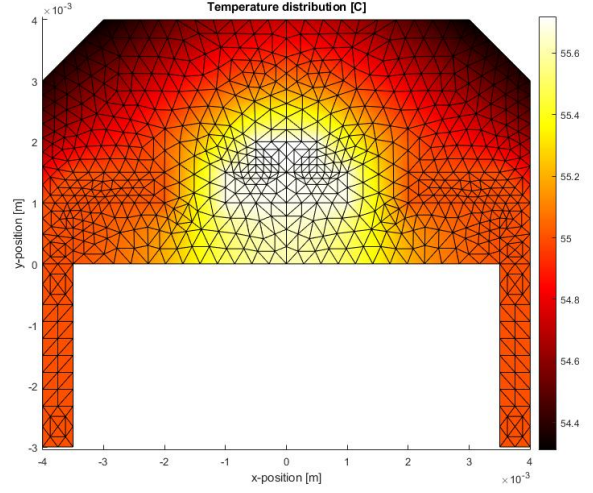
The mesh contains  $n_{el} = 692$  elements and  $n_{nodes} = 386$  nodes.

#### 3.1 Heat flow

The solution to the stationary heat flow problem was obtained by a script in MATLAB (see code appendix) using CALFEM functions. All elements were iterated over in order to calculate the element stiffness matrices  $\mathbf{K}$  and  $\mathbf{K}_c$  which were then assembled according to the mesh into the global stiffness matrix. The equation (12) was then solved using 'solveq' from CALFEM. See results in figure 3.



(a) Full consumption



(b) 25% reduced consumption

Figure 3: Plot of solution to the stationary heat flow problem. All temperatures are in celsius ( $^{\circ}\text{C}$ ) on the color bar to the right of the mesh. Notice the different temperature scales.

The maximum temperature of the stationary solution in figure 3 was approximately  $68.3^{\circ}\text{C}$ , which was in the die of the processor, which is where the heat source is located. The maximum temperature with a 25% reduction in data consumption was approximately  $55.7^{\circ}\text{C}$  in the die.

### 3.2 Transient heat flow

The solution to the transient heat flow problem was obtained iteratively through the implementation of (17) in MATLAB. CALFEM was used to obtain the element matrices  $\mathbf{C}^e$  which were then assembled according to the mesh. A time step of size  $\Delta t = 1$  second were used and the solution was obtained for a period of 20 minutes. Below are plots detailing how the temperature evolved where four different moments in time are shown. The maximum temperature of the solution in each step was also stored and plotted both for the full consumption and the reduced.

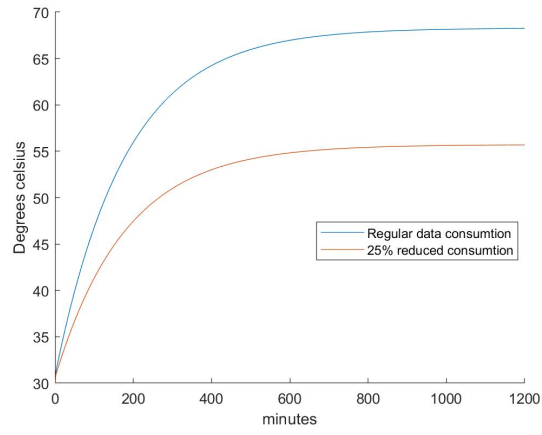


Figure 4: Maximum temperature over time in the chip for full consumption (blue) and 25% reduced consumption (red)

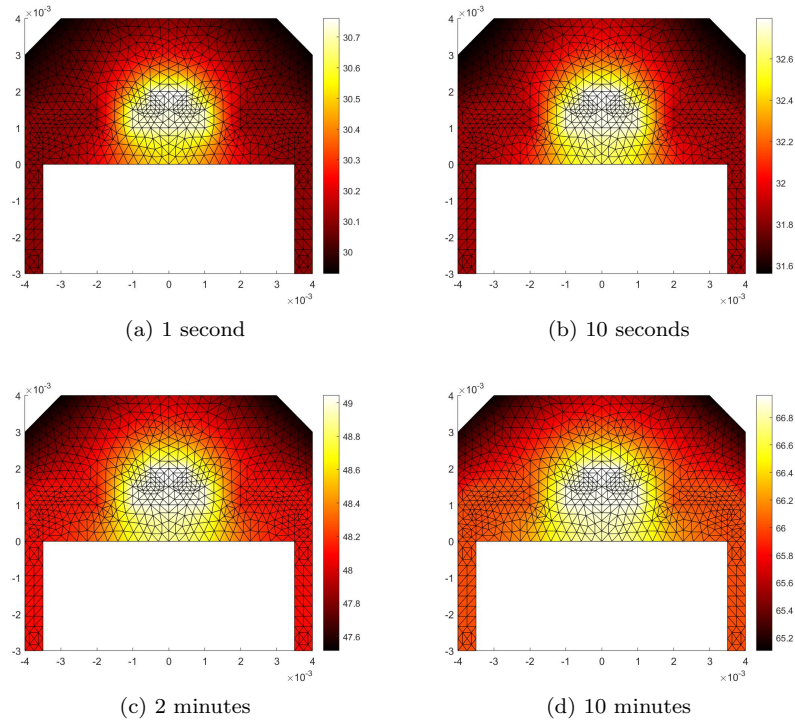


Figure 5: The transient heat distribution in  $^{\circ}\text{C}$  for the times (a) 1 second, (b) 10 seconds, (c) 2 minutes and (d) 10 minutes.

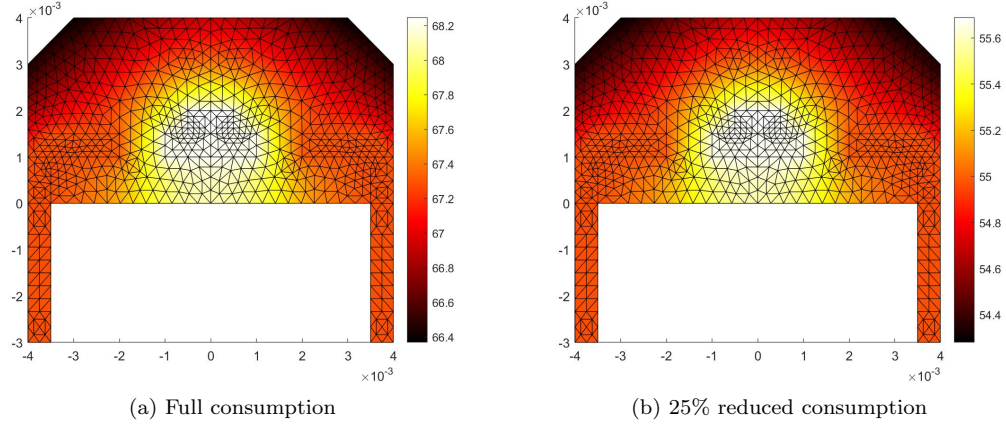


Figure 6: The transient heat distribution in  $^{\circ}\text{C}$  for both full and reduced consumption. Maximum temperatures were approximately 68.2 and 55.7  $^{\circ}\text{C}$  respectively. Notice the different temperature scales on the colorbar.

### 3.3 Stresses and strains

In order to obtain the displacement field the solution to the stationary heat flow problem was first obtained. Appropriate boundary conditions were assigned defined in section 1.1. Using the solution to the stationary heat flow problem the average temperature for each element was calculated and the strains for each element (definition 28) were also found. With this the global stiffness matrix and boundary force vector was assembled analogously to earlier solutions by assembling the respective element matrices and the equation  $\mathbf{K}\mathbf{a} = \mathbf{f}_0$  was solved with the CALFEM 'solveq' function.

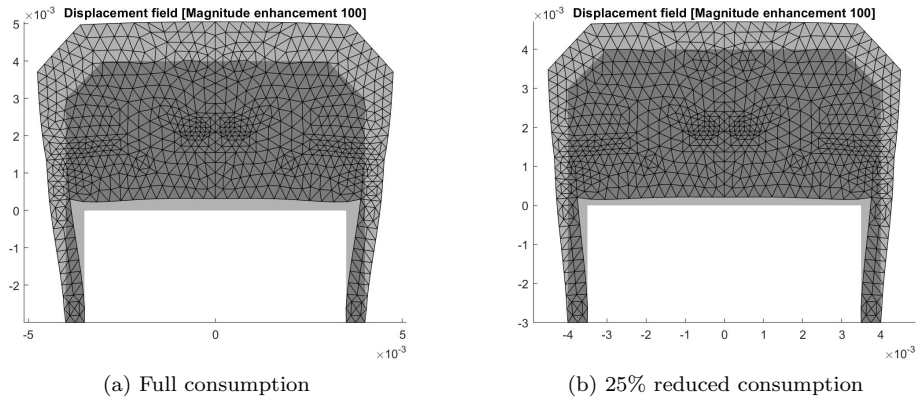


Figure 7: Displacement field for full and reduced consumption

Furthermore the stresses for each element were calculated according to (27) using the earlier displacements and the thermal strains. These were then used to calculate the von Mises

stress field defined by (35), and the stresses in the nodes were calculated by averaging out the stresses in the adjacent elements which resulted in the final stress field.

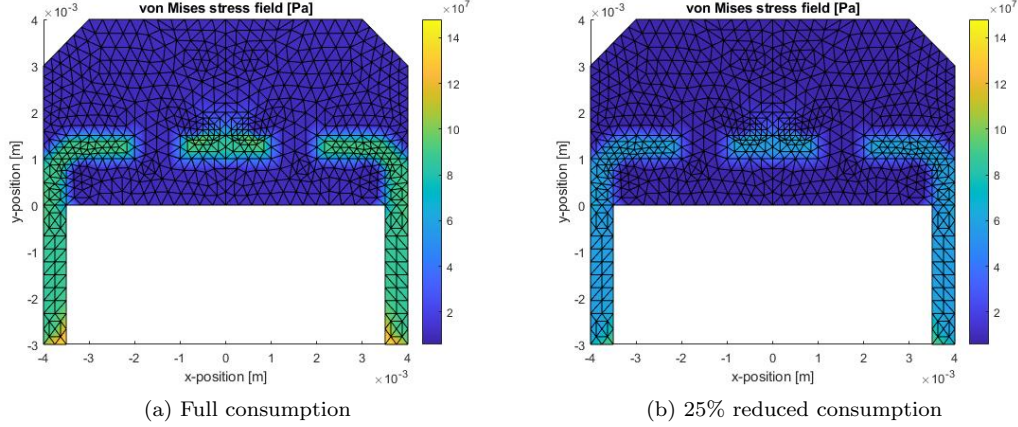


Figure 8: von Mises stress field for different parts of the body. The left part corresponds to full consumption and the right one reduced consumption. The x- and y-axis depict the positions on the chip (in m) and the color value corresponds to the stress in Pa. The stresses are plotted for each element, which have been calculated by averaging out the stresses in the nodes.

The peak stress for full consumption was approximately 148 MPa and 96.9 MPa for reduced consumption. In figure 8 we see that the maximum stress is achieved at the bottom of the copper part of the chip, where it is mounted to the board.

## 4 Discussion

In general, a finer mesh could have been used for greater accuracy. However this of course implies a longer computing time.

### 4.1 Heat flow

The maximum temperature of the stationary heat flow problem was achieved in the die, which naturally corresponds to the fact that this is where the heat source is placed. However, the adjacent copper part which is situated below the die developed temperatures with essentially the same magnitude, compared to the surrounding epoxy material, which were slightly lower. This effect could be the cause of the difference in thermal conductivity, where  $k_{copper} = 385$  compared to  $k_{epoxy} = 5$  W/(m K), where a higher value would correspond to a greater ability to conduct heat.

Comparing the maximum temperature of the body before and after the reduction in data consumption we have that the maximum temperature prior was 68.3 °C and 55.7 °C after. This roughly corresponds to an 18.5 % reduction in maximum temperature. In this case the reduction was percentually smaller than the reduction in data consumption, suggesting that

there is not a linear relation between them. However, such a linear relation might not be what we should expect from such a complicated problem. Additionally, the distribution of the heat is relatively similar for both cases, suggesting that the heat distribution is mainly defined by the structure of the body and its materials rather than the size of the heat source.

Another observation is that the temperature over the copper part that connects the chip to the board has a relatively even temperature, which might be related to the fact that the subsection is made of a homogeneous material with the same thermal conductivity. Lastly the effect of the fan, and therefore also the convection, can be seen on the left and right parts of the top boundary, where the temperature is significantly lower.

## 4.2 Transient heat flow

The maximum temperature achieved in the transient case was 68.2 and 55.7 °C for the full and reduced cases respectively. These temperatures are essentially the same as for the stationary heat distribution, with a difference of 0.01 °C for the case with full consumption. This disparity is assumed to be the result of numerical errors and rounding, or that we simply just need to obtain the solution over a longer time period. In theory the transient heat distribution asymptotically tends towards the stationary distribution, which agrees with the measured maximum temperatures over time in figure 4.

Some minor improvements could be to use a more sophisticated time stepping scheme in order to get better stability, but the chosen scheme is nonetheless sufficient for this type of problem. A smaller time step would also be an improvement for better accuracy, which on the other hand is a tradeoff with respect to computing time.

## 4.3 Stresses and strains

If we consider figure 7 which depicts the displacement field for full and reduced consumption, we see that the displacement in general is smaller in the reduced case, which is as expected. The reduced heat has resulted in less thermal strains since the materials have not expanded as much.

For the stresses in figure 8 the maximum stress for each case was 148 MPa and 9.69 MPa respectively, corresponding an approximate reduction of 35%. The maximum stresses were found at the bottom part of the copper section which connects the chip to the board, i.e  $u_x = 0$ ,  $u_y = 0$ . One explanation to the increased stress might be that because of the inability for the material to expand in those directions reactive forces instead increase the stress in the material.

For copper the stress limit for deformation (yield stress,  $\sigma_s$ ) is 33 MPa. [4] Looking at the maximum stress for both cases, it appears that deformation would occur for both regular consumption and reduced as both maximum stresses exceed the limit.

Ultimately some of the plots could have used a shared temperature scale for easier comparison. However since the heat distribution varies within such small and different intervals it was difficult to achieve a shared scale which depicted the two different distributions well.



## 5 Computer Code

See attached files.

## References

- [1] Niels Ottosen and Hans Petersson. *Introduction to the finite element method*. 1992.
- [2] LTH Division of solid mechanics. Note on transient heat flow fhlf01.
- [3] Mathias Wallin, 2020.
- [4] [http://www.matweb.com/search/datasheet\\_print.aspx?matguid=9aebe83845c04c1db5126fada6f76f7e](http://www.matweb.com/search/datasheet_print.aspx?matguid=9aebe83845c04c1db5126fada6f76f7e).